Environmental modelling of aluminium based components manufacturing routes: Additive manufacturing versus machining versus forming

Validation of the simplified heat conduction model of EN ISO 52016-1

Validation of the simplified heat conduction model of EN ISO 52016-1

G De Luca[1,*], I Ballarini[1], F G M Bianco Mauthe Degerfeld[1] and V Corrado[1]

[1] Department of Energy "Galileo Ferraris", Politecnico di Torino, Corso Duca degli Abruzzi 24, 10129 Turin, Italy

[*] giovanna.deluca@polito.it

Abstract. The issue of improving the building energy efficiency led to the development of calculation methods for the building energy performance assessment. To overcome the low accessibility to detailed input data, the recently introduced EN ISO 52016-1 hourly method is based on assumptions and simplifications chosen to allow a sufficient accuracy in the outcomes with a low amount of input data. Among these assumptions, a simplified mass distribution in the envelope components is considered. In the present work, the hypothesis of the simplified heat conduction model introduced by the EN ISO 52016-1 technical standard and an improved solution provided by its Italian National Annex were evaluated. In particular, the accuracy in the prediction of the internal surface temperature was assessed in comparison with a detailed finite difference conduction algorithm. The validation was performed for 5 opaque component test cases, covering a wide range of areal heat capacity values, by considering both internal and external thermal constraints (e.g. variation of the air temperature). For the structures and boundary conditions considered, results reveal that the standard algorithm allows to predict the internal surface temperatures with a valuable level of accuracy compared to the finite difference algorithm.

1. Introduction

During the last decades, the issue of improving the energy performance of buildings [1] led to the rapid development of different calculation methods for the building energy performance assessment. Several approaches, varying according to the specific purpose or level of accuracy and detail required, can thus be found. However, the current trend of using increasingly detailed methods to obtain accurate results presents an issue due to the low accessibility to detailed input data. To overcome this issue, different simplified dynamic methods, which are based instead on easily retrievable data, were developed. Among them, the recently issued EN ISO 52016-1 hourly method [2] is based on different assumptions and simplifications selected so as to allow a sufficient accuracy with a low amount of input data required [3]. However, the modelling assumptions introduced by this simplified method may lead to inaccurate predictions in the energy consumption of buildings both in design phases and in energy audits. The validation of the simplified method is thus of foremost importance, and the effects related to the introduction of its assumptions need therefore to be investigated.

Since the release of the technical standard in 2017, only a few research studies have addressed the validation of its simplifications and modelling assumptions. Ballarini et al. [4] detected the use of constant surface heat transfer coefficients as the main cause for the differences in the discrepancies between the results of the EN ISO 52016-1 hourly method and the detailed dynamic calculation tool

(EnergyPlus) for a single-family house in Turin (Italy). Zakula et al. [5] tested the accuracy of the new simplified method for several buildings, including different levels of thermal insulation and building uses, and different climatic zones. Their results showed that the simplification introduced by the EN ISO 52016-1 hourly method on the use of fixed windows solar properties leads to significant discrepancies in the outcomes between the simplified method and the detailed hourly method implemented in TRNSYS for most of the considered buildings. In the studies presented, the effect of some modelling options of the EN ISO 52016-1 hourly model on the accuracy of the method was clearly highlighted. However, not all the assumptions introduced by EN ISO 52016-1 have been evaluated in the past studies.

Within this framework, the simplifications on the conduction heat transfer through the building envelope components introduced by the EN ISO 52016-1 technical standard are evaluated in the present study. In particular, the simplified approach of EN ISO 52016-1 for the opaque component discretization into resistive-capacitance nodes and for the mass distribution is investigated, and its accuracy is assessed in comparison with the detailed finite difference conduction algorithm, implemented in the EnergyPlus calculation engine. An improved version of the EN ISO 52016-1 approach, introduced in the Italian National Annex and validated in [6], is evaluated as well. To guarantee a general validity of the outcomes, the validation is performed for five external walls, which covers a wide range of structure heat capacity and mass position. Three different boundary conditions, including both cyclical and realistic variation of indoor and outdoor air temperature are considered.

2. Theory

2.1. The EN ISO 52016-1 heat conduction model

In compliance with the thermal-electrical analogy, the EN ISO 52016-1 heat conduction model considers each building envelope component to be discretised into up to five resistance-capacitance nodes (*R*-*C*). As far as the opaque components are concerned, five *R*-*C* nodes are considered regardless of the specific characteristics and thermal properties of the component, as shown in Figure **1**.

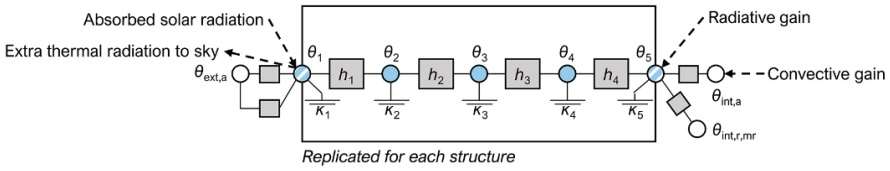

Figure 1. Illustration of the EN ISO 52016-1 *R*-*C* model for an opaque building element

Two nodes are placed on the external and on the internal surface, respectively, while the others are placed inside the construction element. The *R*-*C* nodes are interconnected by four conductances (h_{pli}, with *pli* from 1 to 5), defined in equation (1) as fixed ratios of the total thermal resistance of the component (R_c). In the same way, to each *R*-*C* node is associated a thermal capacity (κ_{pli}), defined as a portion of the total areal heat capacity of the structure (κ_m). Each component is assumed to belong to one of the five mass distribution classes, defined in function of the mass position inside the component, and specified by the technical standard [2] as follows:

- Class I, where the mass is concentrated at internal side,
- Class E, where the mass is concentrated at external side,
- Class IE, where the mass is divided over internal and external side,
- Class D, where the mass is equally distributed (e.g. uninsulated constructions), and
- Class M, where the mass is concentrated inside.

Depending on the assumed mass distribution class, the total areal heat capacity of the structure is distributed over the five *R*-*C* nodes, as shown in Table 1. In addition to the mass distribution classes,

EN ISO 52016 also introduces pre-calculated areal heat capacity values to be used whenever the actual value is unknown. To discard the errors related to the use of different input data, the actual heat capacity values are used in the present work.

$$h_1 = h_4 = \frac{6}{R_c}, \quad \text{and} \quad h_2 = h_3 = \frac{3}{R_c} \tag{1}$$

Table 1. Distribution of the total areal heat capacity of the structure over the *R-C* nodes for each mass distribution class.

Class I	$\kappa_1 = \kappa_2 = \kappa_3 = \kappa_4 = 0, \ \kappa_5 = \kappa_m$	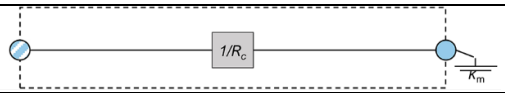
Class E	$\kappa_2 = \kappa_3 = \kappa_4 = \kappa_5 = 0, \ \kappa_1 = \kappa_m$	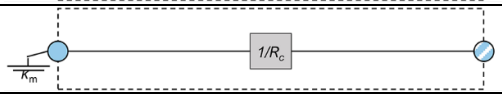
Class IE	$\kappa_2 = \kappa_3 = \kappa_4 = 0, \ \kappa_1 = \kappa_5 = \frac{\kappa_m}{2}$	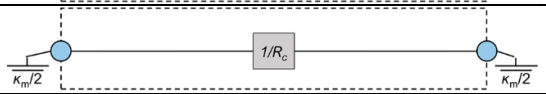
Class D	$\kappa_2 = \kappa_3 = \kappa_4 = \frac{\kappa_m}{4}, \ \kappa_1 = \kappa_5 = \frac{\kappa_m}{8}$	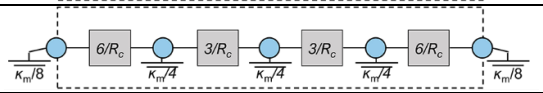
Class M	$\kappa_1 = \kappa_2 = \kappa_4 = \kappa_5 = 0, \ \kappa_3 = \kappa_m$	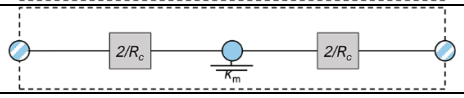

2.2. The EN ISO 52016-1–Italian Annex heat conduction model

The conduction model of the Italian National Annex to EN ISO 52016-1 is an improved version of the one presented in the standard; in particular, it provides a more detailed approach for the opaque components discretization into *R-C* nodes that is more in line with the physical characteristics of the layers composing the structure, as shown in Figure 2.

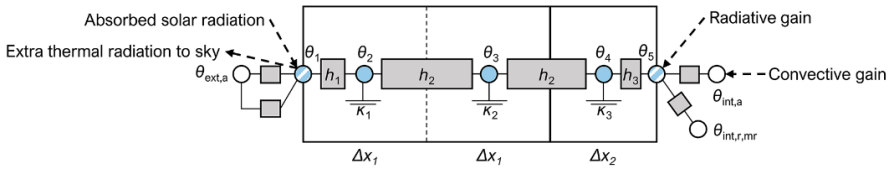

Figure 2. Illustration of the *R-C* Italian Annex model for an opaque building element

As for the EN ISO 52016-1 method, two nodes are placed on the internal and on the external surface, respectively. However, in the improved method, no heat capacity is associated to the surface *R-C* nodes. The main difference between the standard and the improved method is the definition of the number and position of the *R-C* nodes inside the structure. Each layer is in fact discretised into at least one node; the number of nodes (Ncn_j) in the *j*-layer is defined based on a correlation between the Fourier number for the *j*-layer (Fo_j) and a reference Fourier number (Fo_{ref}) assumed equal to 0.5, as defined in equation (2). To each node is associated a ratio of the layer thickness (Δx_j in Figure 2), of the layer heat capacity ($\kappa_{pli,j}$ with *pli* from 1 to Ncn_j), and of the layer thermal resistance ($R_{pli,j}$), defined as in equation (3). The node is placed in the middle of its associated Δx_j. The internode conductances ($h_{pli,j}$ with *pli* from 1 to Ncn_j) are determined considering half of the thermal resistances associated to each node, as defined in equation (4).

$$Ncn_j = \max\left[1; \text{int}\left(\left(\frac{Fo_{\text{ref}}}{Fo_j}\right)^{\frac{1}{2}} + 0.999999\right)\right] \tag{2}$$

$$\Delta x_j = \frac{d_j}{Ncn_j}, \quad \kappa_{pli,j} = \rho_j \cdot c_j \cdot \Delta x_j, \quad \text{and} \quad R_{pli,j} = \frac{\Delta x_j}{\lambda_j} \tag{3}$$

$$h_{pli,j} = \frac{1}{\frac{R_{pli-1,j}}{2} + \frac{R_{pli,j}}{2}} \tag{4}$$

3. Methodology

In the present work the hypotheses of the simplified heat conduction models are evaluated by applying a code-to-code comparison methodology, and a case-study approach was used to facilitate the achievement of the research goals. In particular, five structures, each representing one of the five mass distribution classes [2], were selected for the present analysis. Each structure was simulated with the standard (i.e. EN ISO 52016-1) and the improved (i.e. Italian National Annex) algorithms, and with the Crank-Nicolson (finite difference) solution algorithm taken as the baseline. A 24 hours simulation was performed for each structure in the steady periodic regime. Both the standard and the improved algorithms were implemented by means of a validated Python script, while the Crank-Nicolson algorithm was simulated through the EnergyPlus calculation engine. A specific simulation environment [8] was adopted for a single component simulation in EnergyPlus.

The accuracy of the simplifying modelling assumptions of the standard and the improved algorithms was evaluated by means of the Root Mean-Square Deviation (*RMSD*) of the internal surface temperature compared to the results of the finite difference solution algorithm simulations, as described in equation (5),

$$RMSD = \left(\frac{\sum_{i=0}^{n} \left(\theta_{\text{model}} - \theta_{\text{CondF}} \right)^2}{n} \right)^{\frac{1}{2}} \tag{5}$$

where, θ_{CondF} and θ_{model} are the internal surface temperatures, resulting from the simulations with the finite difference and the standard/improved solution algorithms, respectively, and n is the number of time-steps evaluated.

3.1. Structures and boundary conditions

The selection of the structures to be analysed in the present work was based on the mass distribution classes specified by EN ISO 52016-1; in fact, each structure is representative of one of the five mass distribution classes. Each of the five structures selected corresponds to a typical construction of the Italian existing building stock, and was derived from the UNI/TR 11552 technical report [6]. In Table 2, the selected structures, which are named as the corresponding mass distribution classes, are described and the layers thermal properties are reported. In absence of structures consistent with the mass distribution class in [6] (e.g. Class M structure), an *ad hoc* structure was hypothesised.

To guarantee a general validity of the outcomes, the structures are analysed under three different boundary conditions, as follows:

- *IntC*, with cyclical variation of the indoor air temperature and constant outdoor air temperature,
- *ExtC*, with cyclical variation of the outdoor air temperature and constant indoor air temperature, and
- *SDD*, that represents the summer design day external boundary conditions of a south-facing wall exposed to solar radiation and constant indoor air temperature.

As regards the summer design day boundary condition, the building was assumed to be placed in Rome (Italy), and the effect of solar radiation was considered by means of the sol-air temperature. As

for the internal and external constraint boundary conditions, a unitary amplitude and a 24 h period of variation was considered for the sinusoidal conditions' definition. In all the considered boundary conditions, the structures were assumed to be only exposed to the convective heat transfer. Thus, the effect of the long-wave radiative heat transfer was annulled and neither solar gains nor internal heat gains were considered.

Table 2. Selected structures description.

	Material	d [m]	λ [W m^{-1}K^{-1}]	ρ [kg m^{-3}]	c [J kg^{-1}K^{-1}]	R [m^{2}K W^{-1}]	R_c [m^{2}K W^{-1}]	κ_m [kJ m^{-2}K^{-1}]
Class I	(ext) Plaster	0.02	0.90	1800	1000	-	3.55	472
	Fiberglass insulation	0.12	0.04	30	670	-		
	Concrete panel	0.30	0.58	1400	1000	-		
	(int) Plaster	0.01	0.70	1400	1000	-		
Class E	(ext) Plaster	0.02	0.90	1800	1000	-	3.55	472
	Concrete panel	0.30	0.58	1400	1000	-		
	Fiberglass insulation	0.12	0.04	30	670	-		
	(int) Plaster	0.01	0.70	1400	1000	-		
Class IE	(ext) Plaster	0.02	0.90	1800	1000	-	3.54	380
	Bricks	0.25	0.40	1000	1000	-		
	Wool rock insulation	0.12	0.05	30	570	-		
	Hollow bricks	0.08	0.40 [a]	800	1000	-		
	(int) Plaster	0.02	0.70	1400	1000	-		
Class D	(ext) Plaster	0.02	0.90	1800	1000	-	0.74	224
	Bricks	0.25	0.39	800	1000	-		
	Air gap	0.12	-	-	-	0.18		
	Hollow bricks	0.08	0.40[a]	800	1000	-		
	(int) Plaster	0.02	0.70	1400	1000	-		
Class M	(ext) Plasterboard	0.019	0.20	700	837	-	5.88	110
	Wool rock insulation	0.12	0.04	70	1030	-		
	XLAM panel	0.1	0.12	470	1600	-		
	Wool rock insulation	0.05	0.04	70	1030	-		
	(int) Plasterboard	0.019	0.20	700	837	-		

[a] Equivalent thermal conductivity

3.2. Mass distribution deviation

The evaluation of the different approaches for the structure mass distribution was carried out by means of two specific parameters introduced by the Authors: the "internal areal heat capacity deviation" ($\kappa_{i,dev}$) and the "periodic thermal transmittance deviation" ($Y_{ie,dev}$). Both the parameters allow the numerical assessment of the mass distribution differentiation between a model and the actual component, and are calculated for each of the considered structures. An "artificial" structure, that represents the mass distribution for the considered heat conduction model, is introduced for the calculation of both the parameters. The "internal areal heat capacity deviation" is considered for the validation of the heat conduction models when the structures are exposed to an internal constraint (*IntC* boundary condition), and it is defined in equation (6) as the difference between the internal areal heat capacity for the "artificial" structure ($\kappa_{i,model}$, J·m^{-2}K^{-1}) and for the actual structure (κ_i, J·m^{-2}K^{-1}), calculated according to the EN ISO 13786 technical standard [9].

$$\kappa_{i,dev} = \kappa_{i,model} - \kappa_i \tag{6}$$

The "periodic thermal transmittance deviation" is instead employed when an external constraint is considered (*ExtC* and *SDD* boundary conditions). It is defined in equation (7) as the module of the difference between the periodic thermal transmittance for the "artificial" structure ($Y_{ie,model}$, W·m^{-2}K^{-1}) and for the actual structure (Y_{ie}, W·m^{-2}K^{-1}), both calculated according to the EN ISO 13786 technical standard [9].

$$Y_{\mathrm{ie,dev}} = \left| \vec{Y}_{\mathrm{ie,model}} - \vec{Y}_{\mathrm{ie}} \right| \tag{7}$$

4. Results and discussion

The accuracy of the simplified heat conduction models was assessed with respect to the finite difference solution algorithm. In particular, the analysis of the results was mainly focused on the internal surface temperature, whereas it is involved in the convective and radiative heat transfer, in the thermal balance of the indoor environment. In Table 3, the *RMSD*s of the internal surface temperature of the analysed structures are reported for the standard and the improved algorithms, and for the three boundary conditions, respectively. The *RMSD*s related to the *SDD* boundary condition were normalised to the amplitude of the sol-air temperature variation, to make them comparable to the *ExtC* results.

Table 3. *RMSD* of the internal surface temperature [°C]

Boundary condition	Heat conduction model	Class I	Class E	Class IE	Class D	Class M
IntC	Improved (UNI)	0.028	0.012	0.036	0.026	0.013
	Standard (CEN)	0.298	0.097	0.231	0.032	0.084
ExtC	Improved (UNI)	0.010	0.005	0.001	0.003	0.006
	Standard (CEN)	0.012	0.014	0.011	0.006	0.006
SDD	Improved (UNI)	0.001	0.001	0.001	0.001	0.001
	Standard (CEN)	0.007	0.014	0.011	0.003	0.002

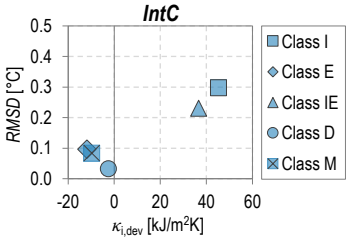

Figure 3. Internal surface temperature *RMSD* vs. $\kappa_{\mathrm{i,dev}}$ for the EN ISO 52016-1 standard conduction model under internal constraint (*IntC*).

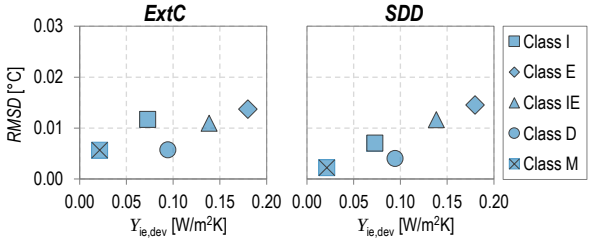

Figure 4. Internal surface temperature *RMSD* vs. $Y_{\mathrm{ie,dev}}$ for the EN ISO 52016-1 standard conduction model under external constraint (*ExtC* and *SDD*).

Generally, the improved solution algorithm introduced by the Italian National Annex ensures very close results to those of the Crank-Nicolson model. As shown in Table 3, negligible values of *RMSD* are reported for all the structures considered, regardless of the thermal constraint stressing the structure. On the other hand, less accurate results can be highlighted for the standard conduction model. To deepen the reasons for these results, it is necessary to separately analyse the structures response when internal (*IntC*) and external constraints (*ExtC* and *SDD*) are considered. To this purpose, in Figure 3 and Figure 4 the *RMSD*s for the standard conduction model are correlated to $\kappa_{\mathrm{i,dev}}$ and $Y_{\mathrm{ie,dev}}$, respectively for the boundary condition *IntC*, and the boundary conditions *ExtC* and *SDD*. From the charts, a linear correlation between the *RMSD*s and the parameters introduced by the Authors can be observed for the considered structures, both under internal and external constraints. In fact, the deviations in the prediction of the internal surface temperatures increase with the increment of the mass distribution deviation. Nevertheless, the accuracy in the prediction of the internal surface temperature is not sensitive to the implementation of the standard conduction model when an external constraint is considered. In fact, negligible deviations (comparable to the improved method results) are reported for both the *ExtC* and the *SDD* boundary conditions. On the other hand, higher discrepancies are reported when the structures are stressed by an internal constraint. In particular, the highest

deviations are relative to the structures characterised by the main massive component placed near the inner side of the structure. Thus, the hypothesis of distribution of the total areal heat capacity on the internal surface *R-C* node (Class I) and half of it (Class IE) leads to an overestimation of the heat capacity effectively stressed by the thermal constraint ($\kappa_{i,dev}$ equal to 45.2 and 36.6 kJ·m^{-2}K^{-1} for Class I and IE, respectively). This overestimation results in considerable discrepancies in the internal surface temperature prediction, with errors in the range of 0.3 °C (i.e. 0.3 °C and 0.23 °C for the Class I and Class IE structures, respectively).

For a better understanding of this last result, the temperature trend inside the structures was analysed. The graphs in Figure 5 represent the *R-C* nodes position inside the structure and the relative temperature at the first calculation time-step (t = 0 h), for the three heat conduction models (black, pink and blue lines for the finite difference, the improved and the standard solution algorithms, respectively).

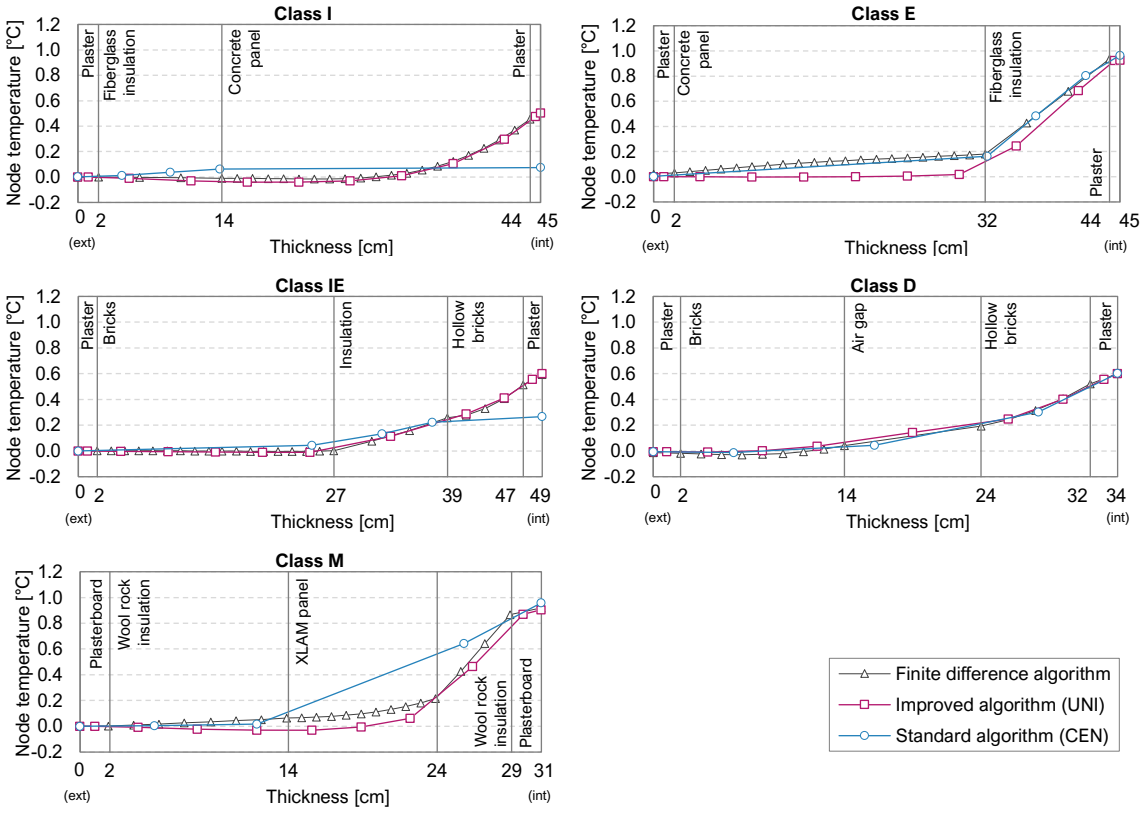

Figure 5. Node temperature comparison (*IntC* boundary condition, t = 0 h)

As far as the Italian approach is concerned, the node temperature analysis confirms the results previously presented. In fact, the temperature trend inside the structure of the improved method is highly consistent with the finite difference algorithm through the whole wall thickness, especially for the Class I, IE, and D structures. Negligible deviations can be instead found for the Class E and M structures, specifically in the massive layers (e.g. the concrete and the XLAM panels, respectively in Class E and M). Moving to the standard model analysis, a very good agreement between the standard and the finite difference algorithm can be found for the Class E and Class D structures. The temperature trend through the wall thickness is in fact highly consistent with the other heat conduction models, resulting in negligible deviations in the prediction of the internal surface temperature (i.e. 0.1 and 0.03 °C *RMSD*s values for Class E and Class D, respectively). With regards to the structures characterised by the massive layers on the inner side (Class I and Class IE), it is possible to observe that the errors in the temperatures mainly occur nearby the nodes on which the structure heat capacity

is distributed (i.e. the internal surface node). This may be due to the fact that the distribution of the whole heat capacity (or half of it) of the structure on the inner surface node leads the inner layers to be less responsive to the temperature variations, with respect to the finite difference and the improved algorithm results, thus resulting in differences in the internal surface temperatures.

5. Conclusions

In the present work, the hypothesis of the simplified heat conduction model introduced by the EN ISO 52016-1 technical standard and the Italian National Annex were evaluated. In particular, the accuracy in the prediction of the internal surface temperature was assessed in comparison with the detailed finite difference conduction algorithm, considering both the internal and the external thermal constraints (i.e. variation of the air temperature).

Generally, the results reveal that the improved algorithm allows to predict the internal surface temperatures with a high level of accuracy, regardless of the thermal constraint considered. Comparable results are reported for the standard method when the structures are stressed by an external constraint. On the other hand, higher discrepancies are highlighted when an internal constraint is considered, especially for the structures characterised by the main massive layer placed on the inner side. Although the reported errors are in the order of 0.3 °C, it is conceivable that higher errors may occur if these structures are exposed to additional driving forces.

Future works will thus be focused in the analysis of the opaque building component response considering additional driving forces, such as internal and solar gains. These further researches will be addressed to increase the accuracy of the simplified dynamic methods and to contribute to the enhancement of the standardization activity.

References

[1] European Commission 2010 Directive 2010/31/EU of 19 May 2010 on the energy performance of buildings (recast)

[2] European Committee for Standardization 2017 Energy performance of buildings - Energy needs for heating and cooling, internal temperatures and sensible and latent heat loads - Part 1: Calculation procedures (EN ISO 52016-1)

[3] van Dijk D 2019 EN ISO 52016-1: The new International Standard to calculate building energy needs for heating and cooling, internal temperature and heating and cooling loads *Proc. of Building Simulation 2019: 16th Conf. of IBPSA* (Rome: International Building Performance Association (IBPSA)) pp 4061-4068

[4] Ballarini I, Costantino A, Fabrizio E, and Corrado V 2020 A Methodology to Investigate the Deviations between Simple and Detailed Dynamic Methods for the Building Energy Performance Assessment *Energies* **13(23)** 6217

[5] Zakula T, Bagaric M, Ferdelji N, Milovanovic B, Mudrinic S, and Ritosa K 2019 Comparison of dynamic simulations and the ISO 52016 standard for the assessment of building energy performance. *Applied Energy* **254** 113553

[6] Mazzarella L, Scoccia R, Colombo P, and Motta M 2020 Improvement of EN ISO 52016-1:2017 hourly heat transfer thought a wall assessment: the Italian National Annex *Energy and Buildings* **210** 109758

[7] UNI Ente Italiano di Normazione 2014 Opaque envelope components of buildings - Thermo-physical parameters (UNI/TR 11552) (in Italian)

[8] Angelotti A, Martire M, Mazzarella L, Pasini M, Baggio P, Prada A, Ballarini I, Corrado V, De Luca G, Bosco F, Cornaro C 2018 Building energy simulation for nearly zero energy retrofit design: the model calibration. *Proc. 2018 IEEE Int. Conf. on Environment and Electrical Engineering and 2018 IEEE Industrial and Commercial Power Systems Europe (EEEIC/I&CPS Europe)* (Palermo: IEEE) pp 1-6

[9] European Committee for Standardization 2017 Thermal performance of building components - Dynamic thermal characteristics - Calculation methods (EN ISO 13786:2017)